

REPORT DOCUMENTATION PAGE

Form Approved
OMB No. 0704-0188

AD-A244 634



is estimated to average 1 hour per response, including the time for reviewing instructions, searching existing data sources, gathering and reviewing the collection of information. Send comments regarding this burden estimate or any other aspect of this collection of information, including this burden estimate, to Washington Headquarters Services, Directorate for Information Operations and Reports, 1215 Jefferson Davis Highway, Suite 1204, Arlington, VA 22202-4302, and to the Office of Management and Budget, Paperwork Reduction Project (0704-0188), Washington, DC 20503.

REPORT DATE
10/11/91

3. REPORT TYPE AND DATES COVERED

Final 15 Mar 91 - 14 Sep 91

5. FUNDING NUMBERS

DAAL03-91-C-0017

INFLUENCE OF PULSED MAGNETIC FIELDS ON
UNIAXIAL STRESS OF FILMS.

6. AUTHOR(S)

C. Vittoria

7. PERFORMING ORGANIZATION NAME(S) AND ADDRESS(ES)

ElectroMagnetic Applications, Inc.
64 Sumner Street,
Newton, MA 02159.PERFORMING ORGANIZATION
REPORT NUMBER

JAN 10 1992

9. SPONSORING/MONITORING AGENCY NAME(S) AND ADDRESS(ES)

U. S. Army Research Office, Code SLCRO-IPO
P. O. Box 12211
Research Triangle Park, NC 27709-221110. SPONSORING/MONITORING
AGENCY REPORT NUMBER

ARO 28417-2-MS-SRI

11. SUPPLEMENTARY NOTES

The view, opinions and/or findings contained in this report are those of the author(s) and should not be construed as an official Department of the Army position, policy, or decision, unless so designated by other documentation.

12a. DISTRIBUTION/AVAILABILITY STATEMENT

Approved for public release; distribution unlimited.

12b. DISTRIBUTION CODE

13. ABSTRACT (Maximum 200 words)

We have developed experimental pulsed field techniques by which stress is considerably reduced in films of $\text{Fe}_{80}\text{B}_{15}\text{Si}_5$. One technique involves the application of a magnetic field of 500 Oe along the hard axis and maintaining the annealing temperature at 275 C. The other technique involves rotation of the film in the presence of the field. We model the reduction in stress in terms of a reduction of defects induced by gas inclusions during film preparation. Our estimate of the stress reduction is in reasonable agreement with other estimates deduced from extended X-ray absorption fine structure (EXAFS) studies. Our studies suggest a systematic experimental technique by which the magnetic anisotropy field can be tailored in a film.

14. SUBJECT TERMS

Magnetic Films, Magnetostrictive Stress, Pulsed Fields.

15. NUMBER OF PAGES

35

16. PRICE CODE

17. SECURITY CLASSIFICATION
OF REPORT

UNCLASSIFIED

18. SECURITY CLASSIFICATION
OF THIS PAGE

UNCLASSIFIED

19. SECURITY CLASSIFICATION
OF ABSTRACT

UNCLASSIFIED

20. LIMITATION OF ABSTRACT

UL

Final Report on the SBIR Project

"Influence of Pulsed Magnetic Fields on Uniaxial Stress of Films"

Contract No. DAAL03-91-0017

(March 15, 1991 - September 15, 1991)

October 11, 1991

Submitted by

ElectroMagnetic Applications, Inc. (EMA)

64 Sumner Street

Newton, MA 02159

Submitted to

US Army Research Office

Research Triangle Park, NC 27709-2211

UNCLASSIFIED

92-00697



92 1 8 088

Final Report

Abstract

We have developed experimental pulsed field techniques by which stress is considerably reduced in films of $\text{Fe}_{80}\text{B}_{15}\text{Si}_5$. One technique involves the application of a magnetic field of 500 Oe along the hard axis and maintaining the annealing temperature at 275°C . The other technique involves rotation of the film in the presence of the field. We model the reduction in stress in terms of a reduction of defects induced by gas inclusions during film preparation. Our estimate of the stress reduction is in reasonable agreement with other estimates deduced from extended X-ray absorption fine structure (EXAFS) studies. Our studies suggest a systematic experimental technique by which the magnetic anisotropy field can be tailored in a film.

Accession For	
NTIS	CRA&I
DTIC	TAB
Unannounced	
Justification	
By	
Distribution	
Availability Codes	
Dist	Availability of Special
A-1	



Introduction

The transition metal-boron film system¹ is recognized as an idealized soft magnetic film system. Films in the amorphous state have relative high resistivity in comparison to permalloy or any other amorphous system. The saturation magnetization can be as high as 80% of that of iron and the magnetic anisotropy field, H_A , is as low as 0.1 Oe. As such, this system lends itself to many useful applications in signal processing,² microwave absorption,³ electronic components,⁴ magneto-optic Faraday rotation devices⁵, and flux-gate sensors.⁶

Typically, films are prepared by the sputtering technique and are found to be amorphous.⁷ Invariably, the films exhibit a well defined easy axis of magnetization in the film plane,⁸ or a uniaxial magnetic anisotropy field, H_A . This has presented a paradox in that amorphous films were thought to be magnetically and mechanically isotropic. We hypothesize that this unique axis of magnetization is induced by stress during the growth of the films. We further hypothesize that both stress and magnetic anisotropies are both uniaxial in symmetry and are connected by the magnetostriction constant, λ . As such, we proposed to investigate one specific film composition in which λ is relative high in comparison to other films within the transition metal-boron alloy system:⁹ $\text{Fe}_{80}\text{B}_{15}\text{Si}_5$. The study entailed the monitoring of H_A as a function of annealing conditions: temperature, magnetic field amplitude and direction, and length of time. The stress amplitude, σ , was deduced from the formula

$$\sigma = (2/3)(M/\lambda)H_A. \quad (1)$$

By measuring H_A before and after annealing the film we calculated the

reduction in stress from Eq.(1) (assuming $\lambda = 32 \times 10^{-6}$). M is measured directly, since it is slightly sensitive to changes in annealing conditions. We find our deduced value of stress reduction is in agreement with an independent measurement of σ by EXAFS studies on films of $\text{Fe}_{80}\text{B}_{15}\text{Si}_5$.^{10,11} It is not clear the mechanism by which the films are stressed during the growth process. However, we surmise that gas inclusions may stress the films in a way to induce an uniaxial stress in the films. Our annealing procedure has reduced the number of defect sites due to gas inclusions.

Film Preparations

Film deposition was performed using an ion Tech beam sputtering gun, mounted in a chamber designed by the Microwave Materials group, and built at Sharon Vacuum Systems (Sharon, MA). The chamber was designed to maintain ultra-high vacuum conditions, and is constructed such that additional ion beam guns and extra diagnostic devices, such as reflection high energy electron diffraction (RHEED) or Auger electron spectroscopy (AES), can be installed. The current diagnostic tool in place is a secondary ion mass spectrometer (SIMS), which can be used either to determine the elemental composition of the residual gases from deposition, or, if used in tandem with an ion gun sputtering a sample, can determine sample composition as a function of thickness. During deposition of the amorphous transition metal films the vacuum system used consisted of an in-line cryopump/mechanical pump combination. Base pressures obtained before deposition were commonly 5×10^{-7} Torr, with a dynamic pressure during deposition of 10^{-4} Torr, principally of purified argon. Deposition rates were typically between 1-2 Å/sec. The thickness of films produced were approximately 3000 Å, with the

typical film produced for the magnetic study being 2500 - 3000 Å thick. The targets used were 3" diameter hot pressed 99.999% purity metal-metalloid powders. The substrates consists of 2"x2" fused quartz, which were rotated at 2 r.p.m. to retard formation of columnar growth. The films were grown at ambient temperature (estimated at 100°C). Film thickness was determined both in situ by means of a quartz thickness monitor, and confirmed by a Dektak thickness profilometer, see Fig.1.

Determination of Annealing Conditions

The aim of this investigation was to reduce the stress in films upon the application of pulsed magnetic fields at high temperature. As such, we performed preliminary annealing experiments to determine the appropriate magnitude of the magnetic field, H , the annealing temperature, and the time duration of the pulsed width. From Fig.2 it is apparent that in this alloy system the highest uniaxial anisotropy magnetic field is about 50 Oe.¹² Thus, a field greater than this value was sufficient to cause alignment for any direction of H in the film plane. We chose the annealing field value to be 500 Oe.

The annealing temperature, T_A , was carefully chosen, since there is a smaller window of temperature range to choose from. The Curie temperature of $\text{Fe}_{80}\text{B}_{15}\text{Si}_5$ is 351°C.¹³ The substrate temperature during growth was $\approx 100^\circ\text{C}$. Thus, $100 < T_A < 351^\circ\text{C}$. We narrowed the choice of T_A by performing the following experiment. We measured the ratio (SQ) of the remanent magnetization to the saturation magnetization as a function of annealing temperature. SQ was measured by applying H along the hard axis of magnetization and monitoring

the magnetization with a vibrating sample magnetometer (VSM). SQ was measured as the temperature was varied continuously in Fig.3. We see from Fig.3 that at about $T_A \approx 230 - 250^\circ\text{C}$ SQ increases significantly which implies that the hard axis of magnetization induced from growth is no longer a hard axis of magnetization, since the magnetization is increased along the hard axis. We chose T_A to be 275°C , since we did not want to exceed the Curie temperature of 351°C .

Finally, the pulse width was determined by applying H in duration of 5, 30, and 60 minutes, while T_A was maintained at 275°C . For example, H was applied for 5 minutes along the hard axis and H_A was measured by VSM technique after the annealing run. After H_A was measured H was applied along the easy axis of magnetization while $T_A = 275^\circ\text{C}$ for the next 5 minutes. At the end of the second annealing run H_A was measured. This was repeated about 5 to 10 times for the 5, 30 and 60 minutes annealing times. In Fig.4 we see that there is little difference in H_A between 5 and 60 minutes annealing times. The important criteria in reducing H_A is the number of cycles or times by which the film is annealed. Hence, we chose five minutes pulsed fields in annealing the films, see Fig.5. It is interesting to note that the saturation magnetization remained relatively constant during these preliminary studies. In summary, the annealing conditions were as follows: $T_A = 275^\circ\text{C}$, $H \approx 500$ Oe, and $\Delta t = 5$ minutes; H was applied along the hard axis of magnetization during the annealing run or cycle.

In addition we have introduced an alternative annealing technique in which H was fixed in magnitude and applied in the film plane, but the film was rotated at an angular frequency of $\omega = 0.62$ rad/sec. The annealing

temperature was fixed at 275°C, see Fig.6. The rationale for this annealing procedure was based upon the notion that any direction in the film plane can be induced to be an easy axis of magnetization including the hard axis (as illustrated from the first annealing procedure).

Experimental Results

A) Annealing Studies - Pulsed Fields

In the torque magnetometer measurement the vertical axis is the torque exerted by the external field on the magnetization, see Fig.7. The vertical axis is in units of dyne-cm and is zero for the field parallel to the easy axis of magnetization. The main feature to note here is that the torque exhibits 180° symmetry or uniaxial symmetry. Indeed, the family of films deposited by us exhibit uniaxial symmetry for the field in the film plane.

In a typical vibrating sample magnetometer measurement the vertical axis is the magnetization component as measured along the field (in unit of emu), see Fig.8. In order to change the unit to proper recognizable units the vertical scale is multiplied by $4\pi/v$, where v is the volume of the film. The horizontal axis is H in units of Oe and it is applied along the hard axis (at 90° away from the easy axis). From Fig.8 only M_s may be obtained. In order to obtain H_c and H_A we needed to expand the scales as shown in Figs.9 and 10. Thus, from Fig.9 we deduced $4\pi M \approx 14.5$ KG, $H_A \approx 12-14$ Oe and $H_c \approx 0.43$ Oe.

On another sample, Fig.10, we obtained H_A and was about 12 Oe and $4\pi M$ was ≈ 14.5 KOe, but $H_c = 0.77$ Oe. In Fig.11 we show a similar plot after

annealing the sample in a pulsed field. The change in H_A due to the annealing procedure is indeed remarkable. H_A is considerably reduced. We measured it to be approximately 1 ~ 2 Oe. This suggests a 10/1 reduction of H_A . Previous annealing studies were only able to reduce at most H_A by 20-30%. We believe that the difference may be due to the reversing of polarity of H during the annealing cycle rather than pulsating the field from 300 down to 0 Oe as in previous work. The saturation magnetization remained approximately the same before and after our annealing procedure. This implies that the film is still amorphous and some magnetic separation has occurred in agreement with EXAFS studies. The remanence magnetization is 92% of the saturation magnetization. The reader is reminded that this direction was the hard axis of magnetization prior to annealing the film in a pulsed mode. These results are repeatable for a given film as well as on other films of the same composition. Finally, the coercive field, H_C , has increased from 0.76 to 2.1 Oe upon annealing of the film. On other films of the same composition the increase is from 0.44 to 2.1 Oe. The increase in H_C may represent an increase in the correlation length of the iron ions as in local "clusters" found in amorphous films or simply due to magnetic separation occurring during the annealing. EXAFS studies^{10,11} do reveal an increase in the correlation number and length with increasing temperature.

B) Annealing Studies - Sinusoidal Fields

In Fig.12 we plot the magnetization (in emu) as a function of H along the hard axis before annealing the sample. The direction of the easy axis is determined after the growth of the film. We measured H_A to be 14 ± 1 Oe. The coercive field, H_C , was measured to be 0.4 Oe. It is understood that this sample was a virgin sample. The corresponding torque measurement is shown in

Fig.13, exhibiting the usual two fold symmetry described above. In Fig.14 we repeat the VSM measurement after annealing the sample under the following conditions:

$$T_A = 275^{\circ}\text{C}$$

$$H = 500 \text{ Oe}$$

$$\omega = 0.62 \text{ rad/sec.}$$

We measured in Fig.14 H_A to be 2 ± 0.5 Oe. The coercive field was 2.67 Oe. In Table 1 we compare the results of this annealing procedure with the pulsed field annealing procedure.

The saturation magnetization remained approximately the same before and after the annealing procedure (0.78 versus 0.77 emu). However, the squareness ratio SQ was greatly affected by either annealing procedure. The other quantities which were greatly affected were H_A and H_C . Based upon the results presented in Table 1 both annealing procedures are effective in reducing H_A . This presents a unique opportunity in being able to process thin film materials for special engineering applications. For example, the technique involving rotation may be deployed during the growth of the film - in-situ annealing. The pulsed field technique may be deployed as a post annealing procedure. As such, it may be possible to tailor a given film of various alloy composition to reduce or increase H_A systematically by these annealing procedures.

C) Related Measurements

In Table 2 we show the results of the ferromagnetic resonance (FMR) data. Of particular interest to us is the zero field FMR (ZFMR). By zero field we mean that there is no external field applied to the magnetic film.

Usually, FMR experiments require a bias external field. We have developed¹⁴ the ZFMR technique using a slot-coplanar device. For films like ours the ZFMR is given below:

$$f = \gamma(H_A 4\pi M)^{1/2}, \quad (2)$$

where

$$\gamma = 2.8 \times 10^6 \text{ Hz/Oe}$$

$$H_A \approx 12 \text{ Oe}$$

$$4\pi M \approx 14.5 \text{ KOe.}$$

H_A and $4\pi M$ are obtained from VSM measurements. The value of γ is obtained from previous work. In fact, there are no adjustable parameters in estimating f in Eq.(2). We estimate f to be 1.21 GHz, whereas the measured value varied between 1.01 and 1.12 GHz.

Besides zero field FMR we have performed standing spin wave mode resonance (SWR) before and after annealing. Fig.15 shows a typical SWR spectrum. The most intense line is the main Kittel line. The weaker lines are the spin wave modes and each excitation is assigned a spin wave order number, n . The dispersion follows the Kittel law

$$\frac{\omega}{\gamma} = H_1 + \frac{2A}{M} \left(\frac{\pi}{d}\right)^2 n^2, \quad (3)$$

where $H_1 = H - 4\pi M$, $\omega = 2\pi f$, f = operating frequency = 9.53 GHz, $\gamma = 2.93 \times 10^6 \text{ Hz/Oe}$. By plotting H versus n , the value of the exchange stiffness constant is obtained. However, the most pronouncing fact is the FMR line above the Kittel line. It implies segregation of some form, since it exhibits resonance. In essence, this data is in agreement with an H_c dependence on annealing, see Fig.15.

Discussion and Conclusions

We propose a simple model which assumes that the local atomic order originates from that of the crystalline equivalent phase(s) except that there is no coordination between sites separated by as much as 10 Å. In addition, the model assumes that although the local symmetry may be known, the occupation number may vary from site to site. EXAFS measurements provided us with a measure of the average distance between magnetic ions and their respective neighboring coordination numbers. EXAFS information^{10,11} is sufficient for us to predict fundamental properties of the Fe₈₀B₁₅Si₅ alloy system.

Saturation Magnetization

In calculating M_s we basically count the number of Fe magnetic ions inside a coordination sphere having radius r as measured by EXAFS. For example, in Table 3^{10,11} the coordination number is ≈ 10 Fe ions within a sphere of radius 2.7 Å relative to a central Fe ion. Thus, the magnetization may be approximated by

$$M_s \approx M_{Fe} (n_o/n_{Fe})(r_{Fe}/r_o)^3, \quad (4)$$

where

$$M_{Fe} = 1740 \text{ G},$$

$$n_{Fe} = 14,$$

$$r_{Fe} = 2.866 \text{ Å},$$

$$n_o = 10,$$

$$r_o = 2.7 \text{ Å}.$$

In the above data M_{Fe} , n_{Fe} , and r_{Fe} are obtained from crystalline Fe data and values of n_o and r_o are measured by EXAFS on Fe₈₀B₁₅Si₅, see Table 3. Substituting above values into Eq.(4) we estimate M_s to be ≈ 1490 Oe. This

should be compared with a measured value of 1450 Oe.

Curie Temperature

From molecular field theory the expression for the Curie temperature (T_c) is

$$T_c = 2Jz\langle s \rangle(\langle s \rangle + 1)/3k_B, \quad (5)$$

where $z = 3.5 \pm 1$ is the first nearest neighbor number measured by EXAFS, $\langle s \rangle = S_{Fe}(n_O/n_{Fe})$, $J = 2.16 \times 10^{-14}$ ergs, $S_{Fe} = 1.1$, and $k_B = 1.38 \times 10^{-16}$ erg/°K is the Boltzmann's constant. We obtain an estimate of 515 K (± 150 K) for T_c . The measured value is 624 K. The reader is reminded that the error associated with such calculations is significant due to the relative uncertainty associated with the measurement of z by EXAFS.^{10,11}

Anisotropy Field

There are three potential sources of uniaxial anisotropy field. The first source is due to the strain arising from a mismatch in thermal expansion coefficients between the substrate materials and the film. The uniaxial axis is typically normal to the film plane in these alloy films, since the stress or strain in the film plane is isotropic. The easy axis of magnetization is either in the film plane (all directions being equal) or normal to the film plane. This type of induced anisotropy field, H_A^\perp , manifests¹⁷ itself as a lowering or raising of the effective magnetization of the film ($4\pi M_s \pm H_A^\perp$). VSM measurements for H in the plane are not sensitive to H_A^\perp .

The second source of uniaxial anisotropy is due to the incomplete occupancy of all sites by Fe ions. For example, if one were to assume the

local symmetry (with 10 Å distance) is of a body-centered type where some ions are missing, it can be shown by simple application of the pair ion model¹⁸ that this leads to a net contribution to the uniaxial anisotropy field. However, if the magnetic correlation between local sites is small and if the number of ions and the vacant sites are random from unit cell to unit cell this source of anisotropy field averages to zero over the entire film. One way of measuring such a local field would be to utilize a probe of sufficient sensitivity to magnetic fluctuations over small regions (~ 10Å). We do not believe that EXAFS^{10,11} is sensitive to this type of local fluctuations in these materials.

Finally, it is well known that gas inclusions are incorporated in the film during processing. Typically, both working (argon) and residual (e.g. nitrogen, hydrogen, and oxygen, etc.) gases are entrapped in the film. The only assumption we make is that the entrapment of the gases establishes an anisotropic network of voids (or defects) in the film. The entrapment of these gases generate strain in the film plane. Relaxation occurring along the axis normal to the film plane is assumed to be negligible. Once a uniaxial stress or strain axis is established to be in the film plane there corresponds¹⁹ an anisotropy field, H_A^{\parallel} , of the following amplitude

$$H_A^{\parallel} = 3\lambda\epsilon\mu/2M, \quad (6)$$

where

$$\mu = 0.8 \times 10^{12} \text{ dyn/cm}^2 \text{ (Ref.20),}$$

$$\lambda_s = 32 \times 10^{-6} \text{ (Ref.9)}$$

$$M = 1450 \text{ G} \quad \text{(measured by us),}$$

$$\epsilon = 0.001 \quad \text{(Refs.10, 11).}$$

Using these parameters our estimate of H_A^{\parallel} is 30 Oe for $\text{Fe}_{80}\text{B}_{15}\text{Si}_5$ compared

to a measured value of 13 to 15 Oe. We surmise that the effect of annealing is to reduce the number of trapped voids in the film during structural relaxation. In Table 4 comparisons between calculated and measured magnetic parameters are shown.

In summary we conclude

- 1) We believe that this is the first study to apply EXAFS measurements to correlate changes in local atomic structure to changes in magnetic properties. Such studies are invaluable in determining the response of materials to practical processing techniques such as annealing and in gaining insight to the fundamental relationship between structure and magnetism.
- 2) We believe that our annealing procedure involving pulsed fields which changing polarity (every five minutes) is an effective procedure to reduce the growth induced anisotropy fields in amorphous magnetic films and therefore stress in the films. The fact that VSM and FMR measurements are in agreement implies that indeed the measurements of H_A by VSM are reliable and consistent with other type of magnetic measurements.
- 3) We have developed an alternative annealing technique which is as effective as the pulsed field technique in reducing H_A . We believe that both annealing techniques may be applicable to the iron-boron alloy to reduce stress. Hence we suggest a systematic procedure by which H_A can be tailored to specific requirements or specifications.

References

1. P. Duwez and S.C.H. Lin, J. Appl. Phys., 38, 4096 (1967).
2. Tagielinski, Mat. Sci. Eng. B3, 467 (1989).
3. S. A. Oliver, V.G. Harris, J. Ryu, and C. Vittoria, IEEE Trans. Magnetism, Mag-25(5), 3355 (1989).
4. H. Warlimont, Mat. Sci. Eng. 99, 1 (1988).
5. G. E. Fish, Mat. Sci. Eng. B3, 457 (1989).
6. O. V. Nielsen, B. Hernando, and F. Primdahl, J.M.M.M. 83, 405 (1990).
7. H. J. Guntherodt and H. Beck, Glassy Metals, Vol. I and II, Springer-Verlag, Berlin, 1983.
8. V.G. Harris, S.A. Oliver, W.B. Nowak and C. Vittori, J. Appl. Phys. 67(9), 5571 (1990).
9. R. C. O'Handley, Phys. Rev. B18, 930 (1978).
10. V.G. Harris, S.A. Oliver, W.B. Nowak, and C. Vittoria, IEEE Trans. Magnetism, Mag-26(5), 1459 (1989).
11. V.G. Harris, to be published in IEEE Trans. Magnetism.
12. V.G. Harris, S.A. Oliver, W.B. Nowak, and C. Vittoria, J. Vac. Sci. Tech. A. 8(3), 1325 (1990).
13. V.G. Harris, Ph.D. Thesis, Northeastern University, unpublished, 1990.
14. J. Ryu, Y. Huang, and C. Vittoria, J. Appl. Phys. 63, 4315 (1986).
C. Vittoria, "Tunable Microwave Filters Utilizing a Slotted Line Circuit and Ferrite Elements", Patent No. 4,590,448.
15. C. Kittel, Phys. Rev. 110, 1295 (1958).
16. S. Chikazumi, "Physics of Magnetism", John Wiley & Son, New York, 1964.
17. R.F. Soohoo, "Magnetic Thin Films", Harper and Row, New York, 1965.
18. Z. Neel, J. Phys. Radium 15, 225 (1954).
19. C. Vittoria and P. Labitz, J. Appl. Phys. 58, (1980).

20.M. J. Sinnott, "The Solid State For Engineers", John Wiley and Sons,
London, 1958.

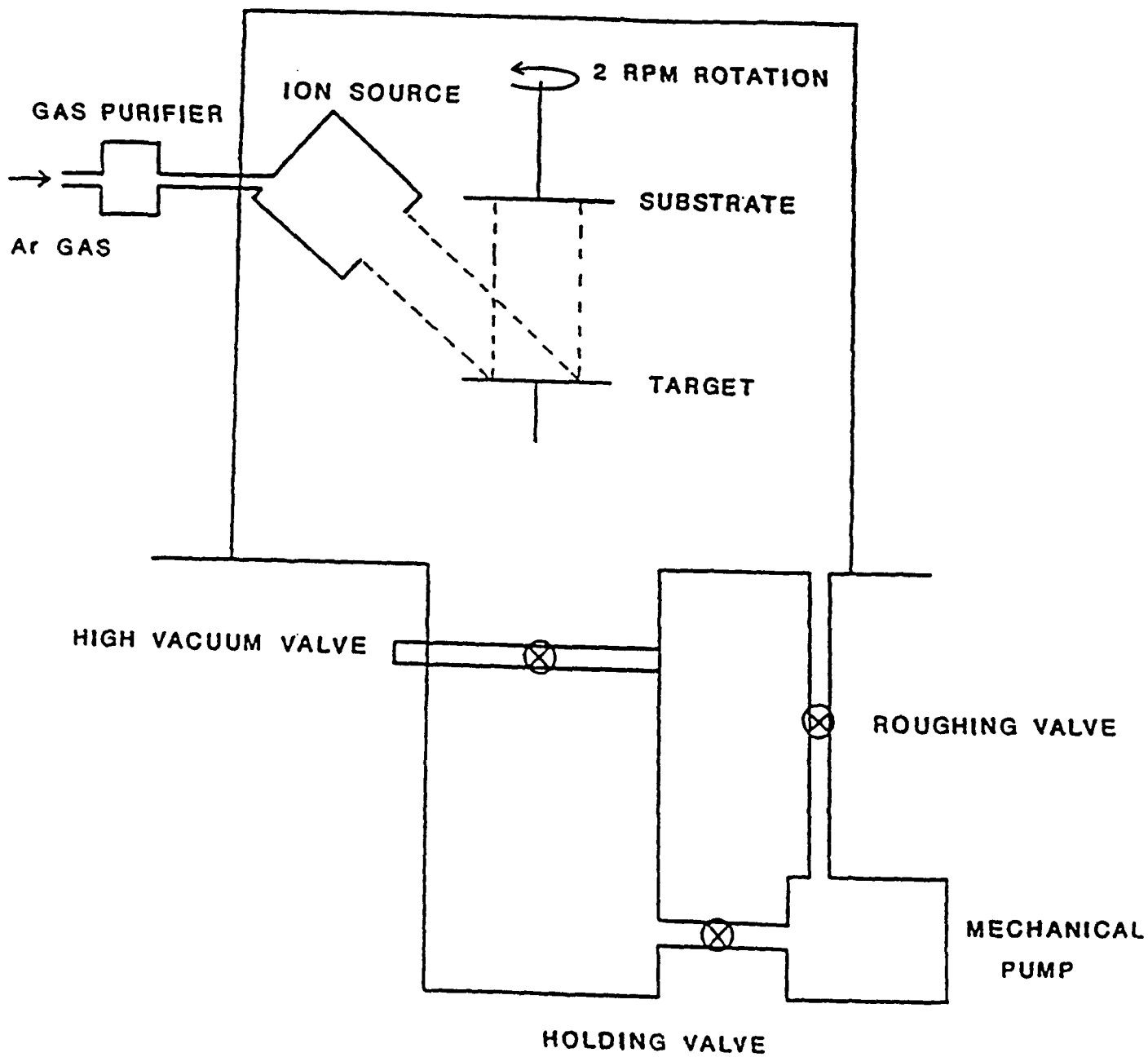


Fig.1 Ion beam sputtering system.

Fe-Ni-Co-B-Si
 H_A (Oe)

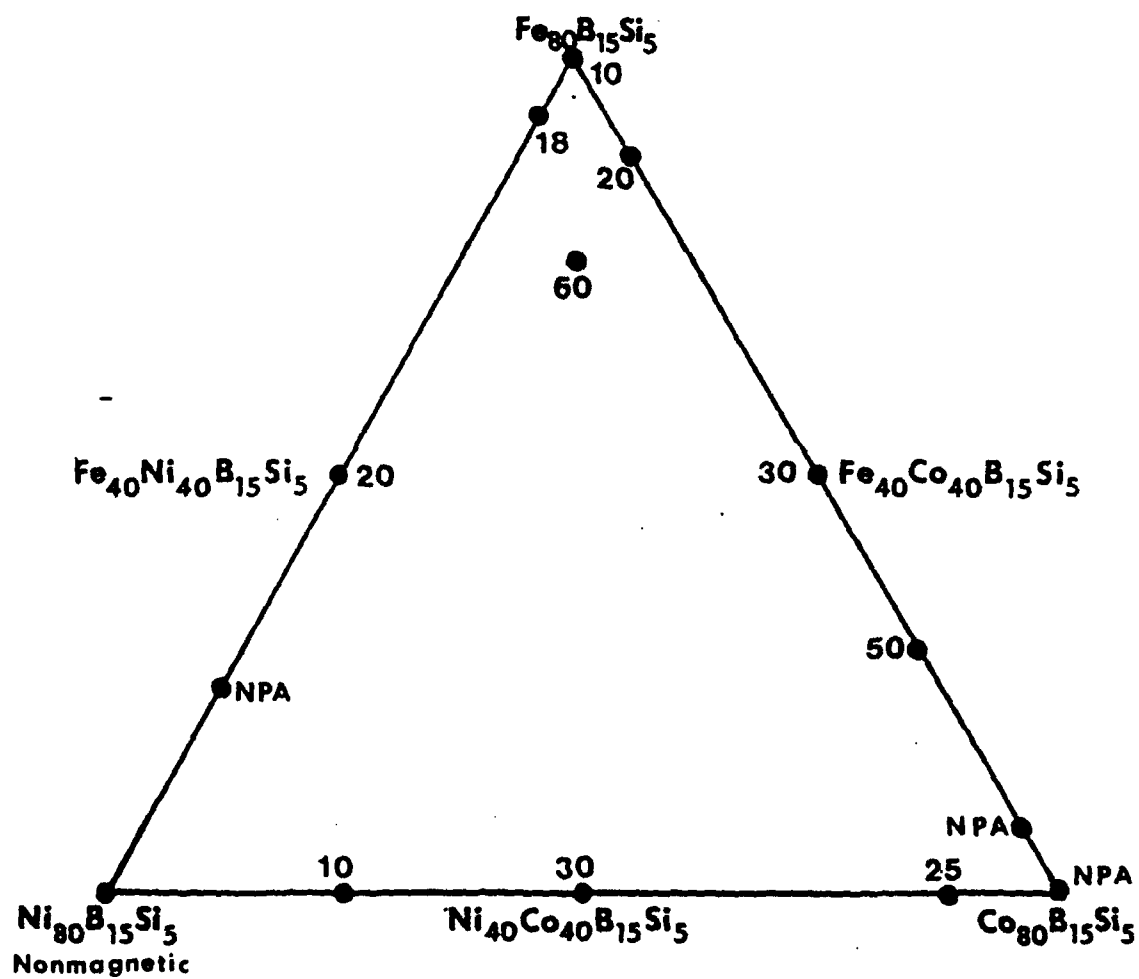


Fig.2 Uniaxial magnetic anisotropy field, H_A , in the Fe-Co-Ni-B-Si System.

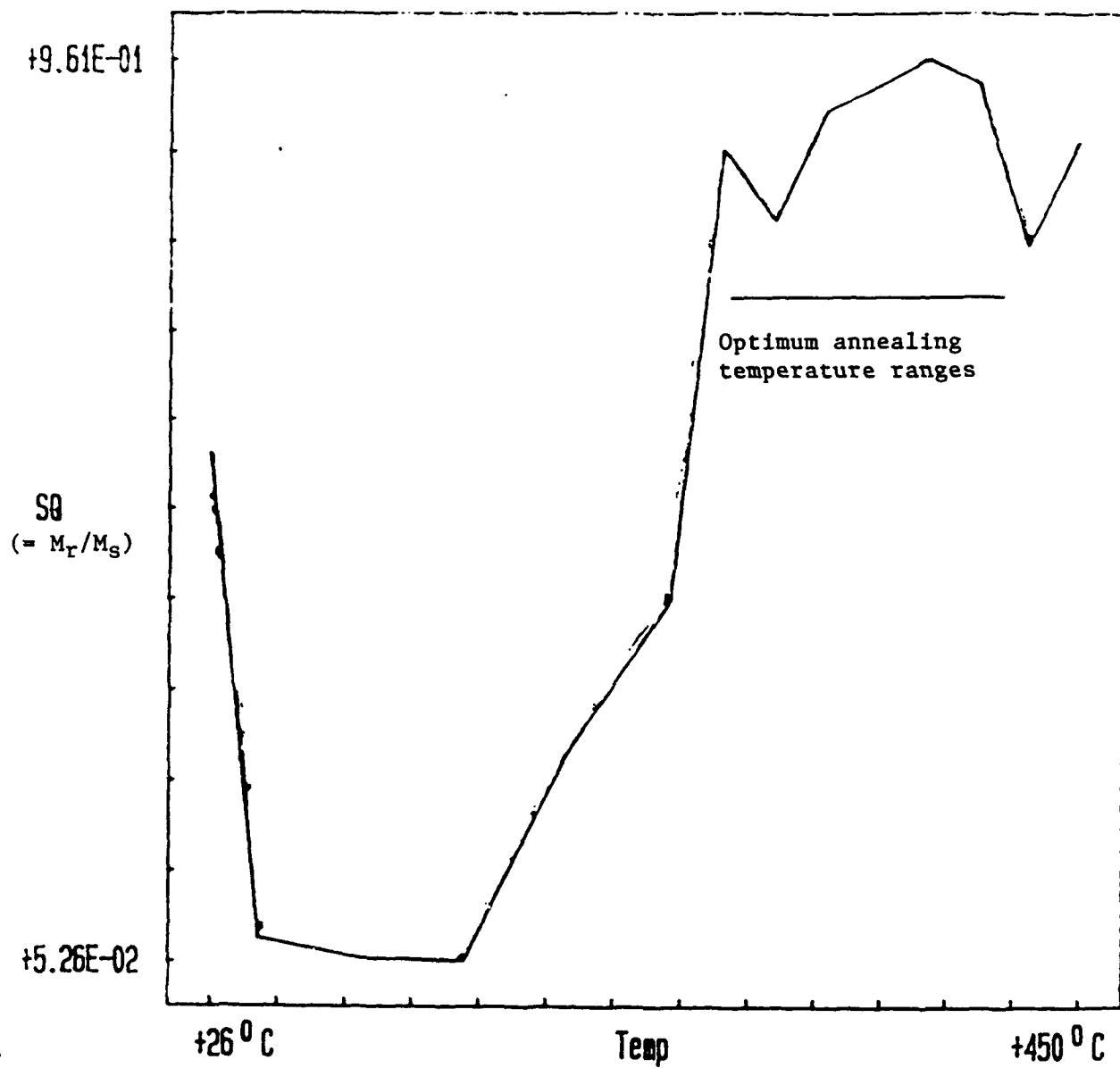


Fig.3 SQ is measured as a function of annealing temperature. SQ is defined as M_R/M_S , where M_R is the remanence magnetization and M_S is the saturation magnetization.

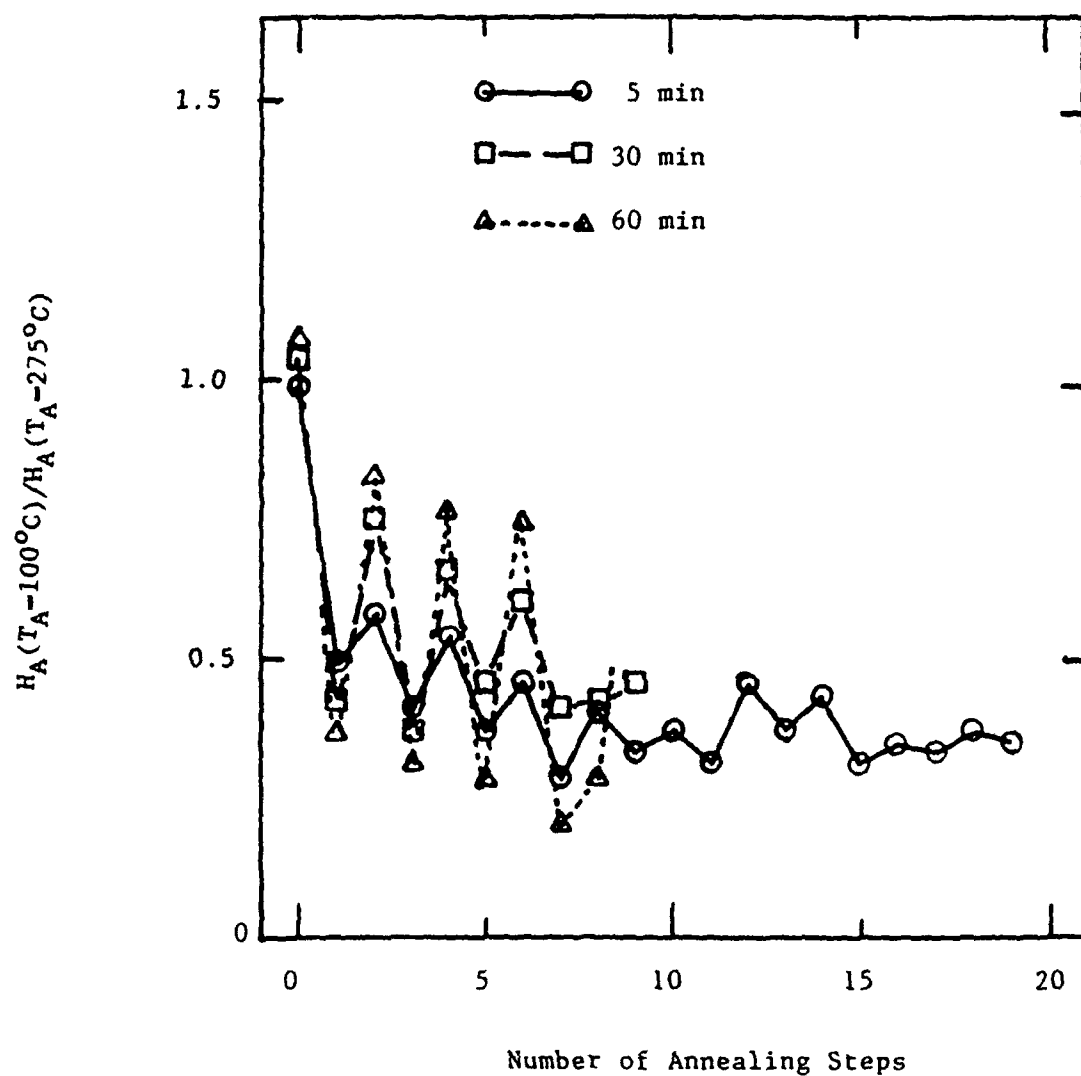
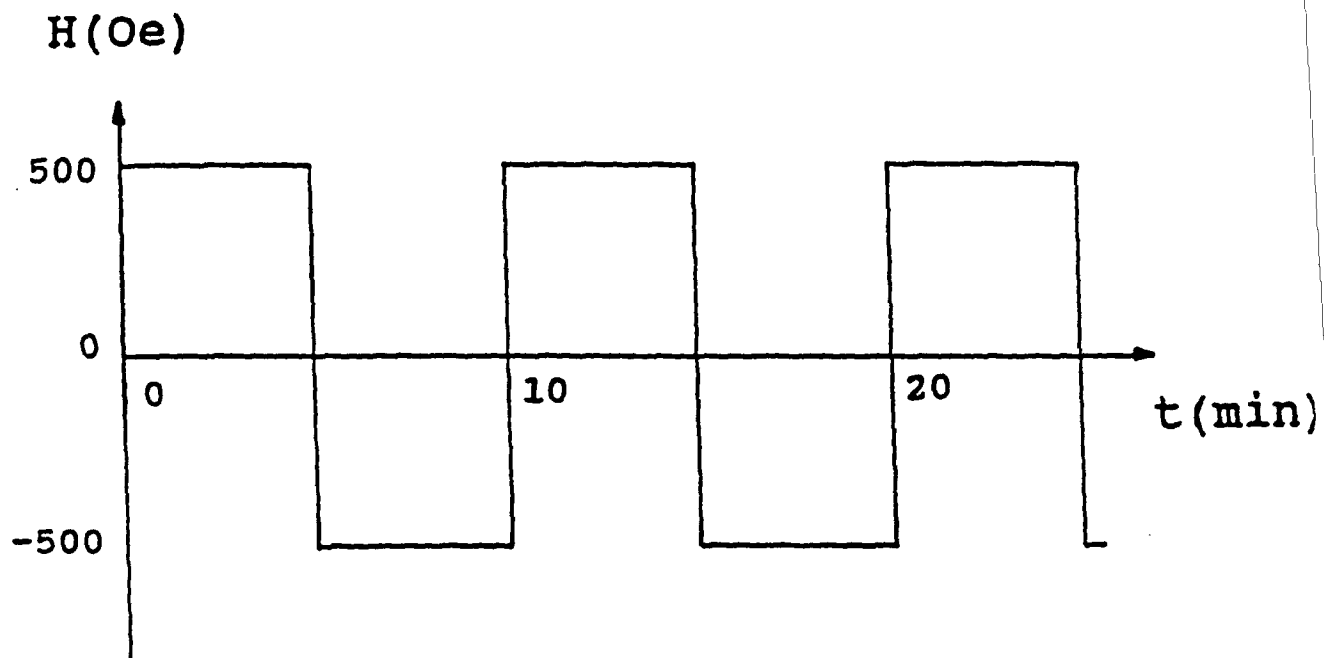


Fig.4 Normalized anisotropy field is plotted as a function of the number of times the film is annealed. The external field is firstly applied along the hard axis for X minutes and then along the easy axis for the same amount of time, where X is the length of time (5, 30, 60 minutes).

a)



b)

Easy Axis

(Film Plane)

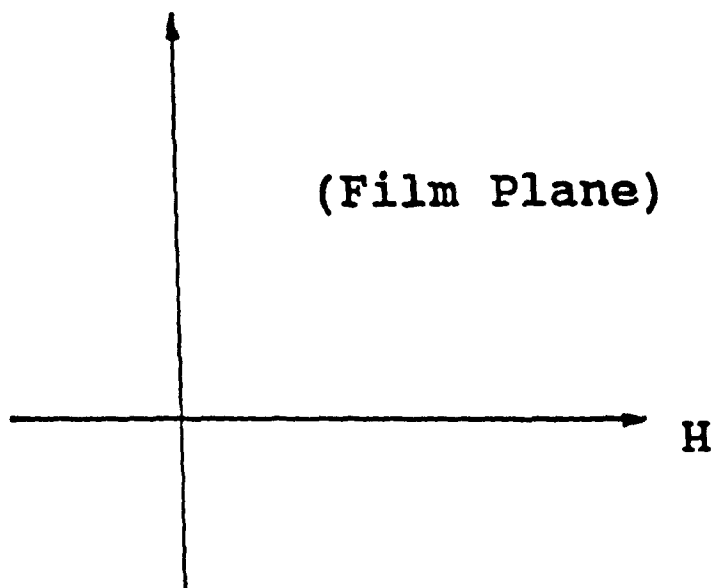
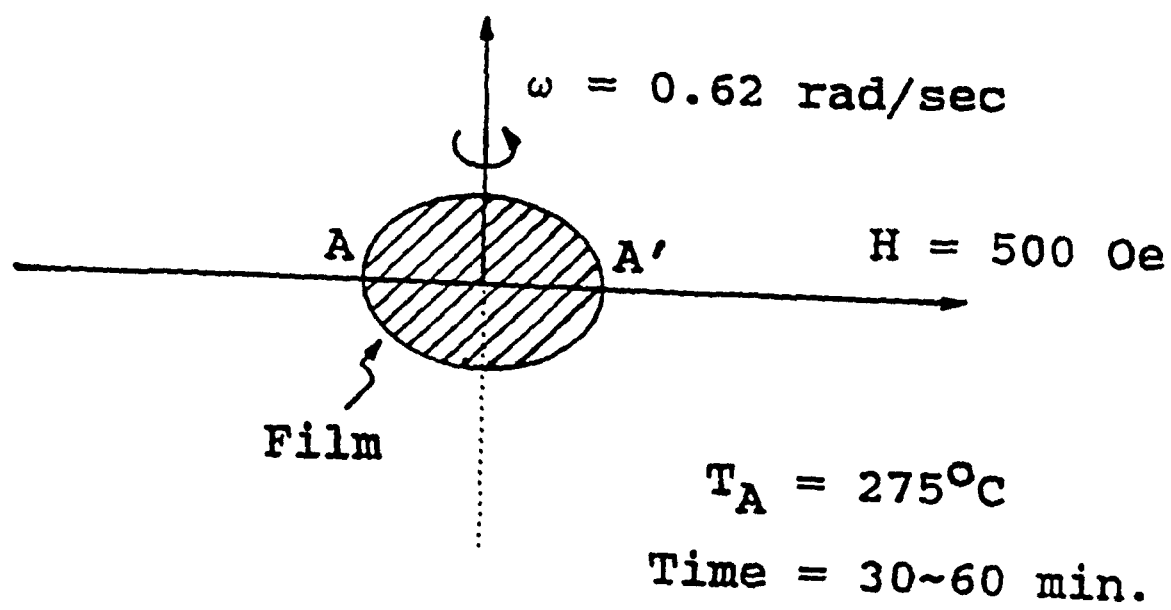
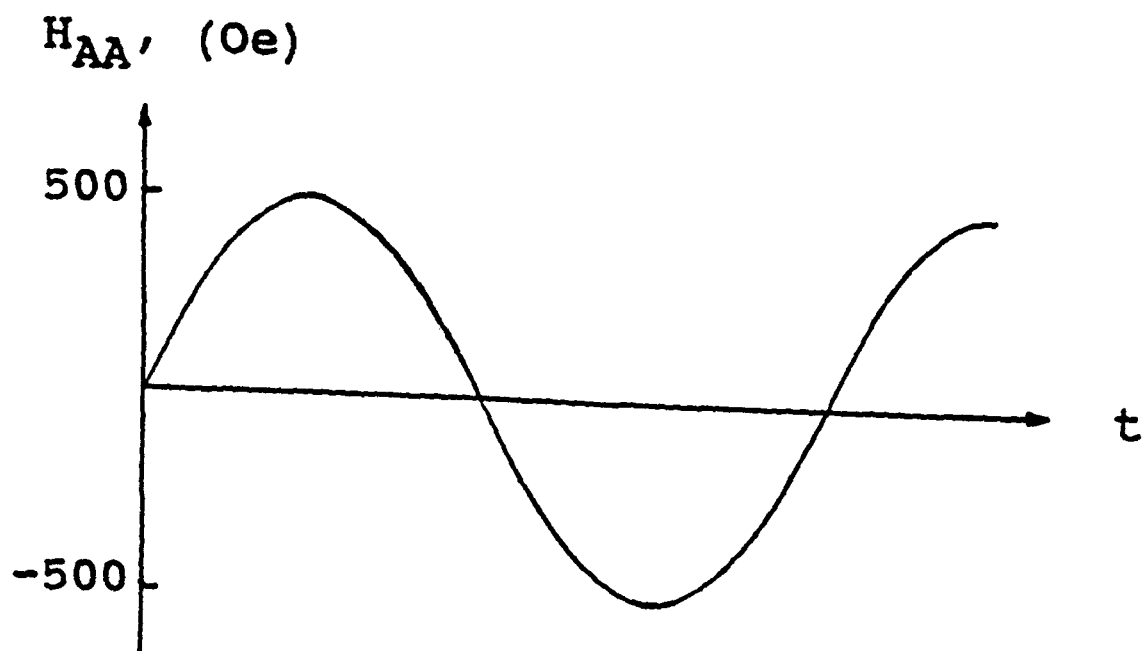


Fig.5 Application of the external magnetic field along the hard axis as a function of time.



(a)



(b)

Fig.6 Application of external magnetic field in the film plane as a function of time.

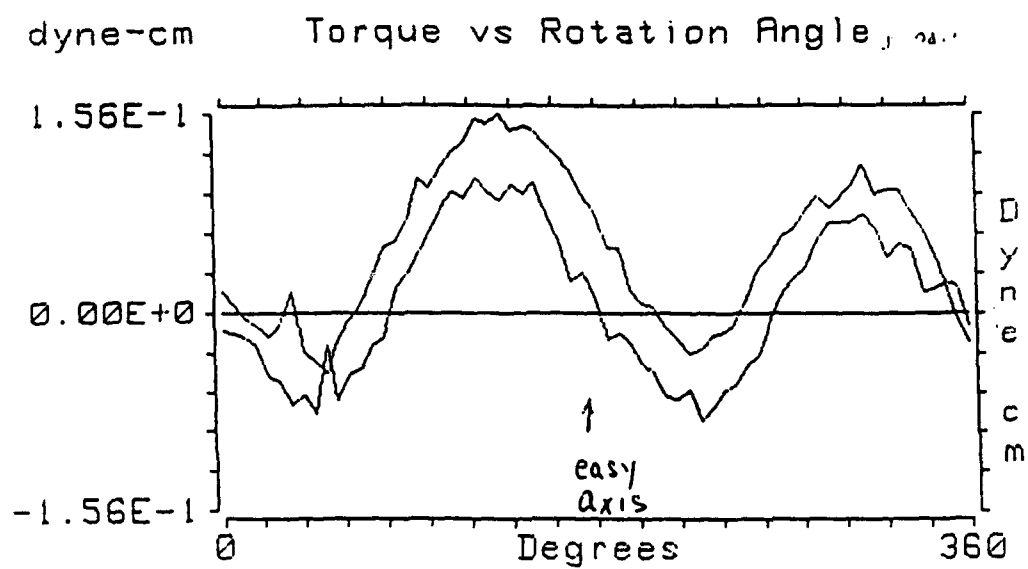


Fig.7 Torque versus angular variation of the in-plane magnetization.

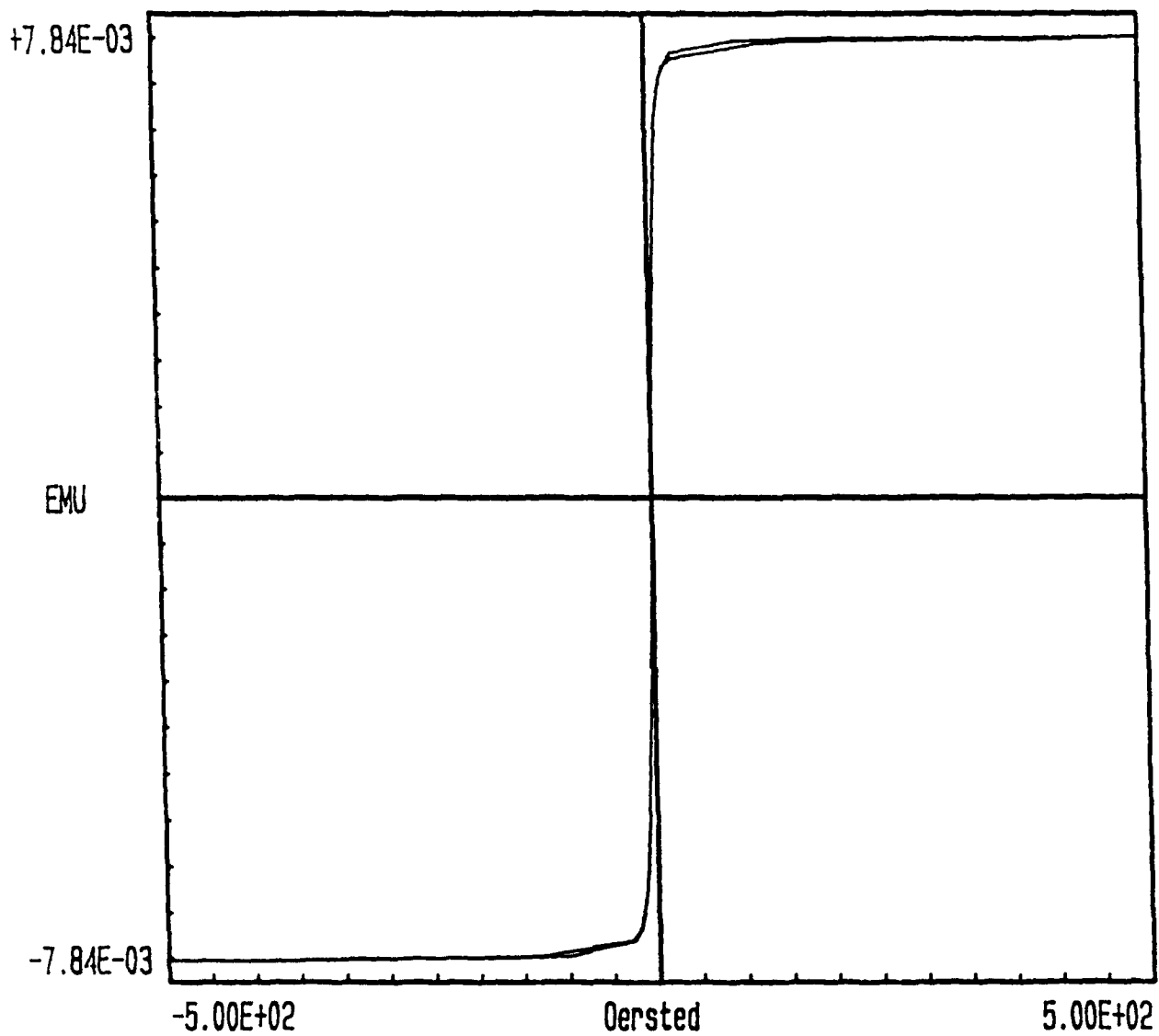


Fig.8 The magnetization as measured along the external field, H, is plotted as a function of H for H along the hard axis of magnetization.

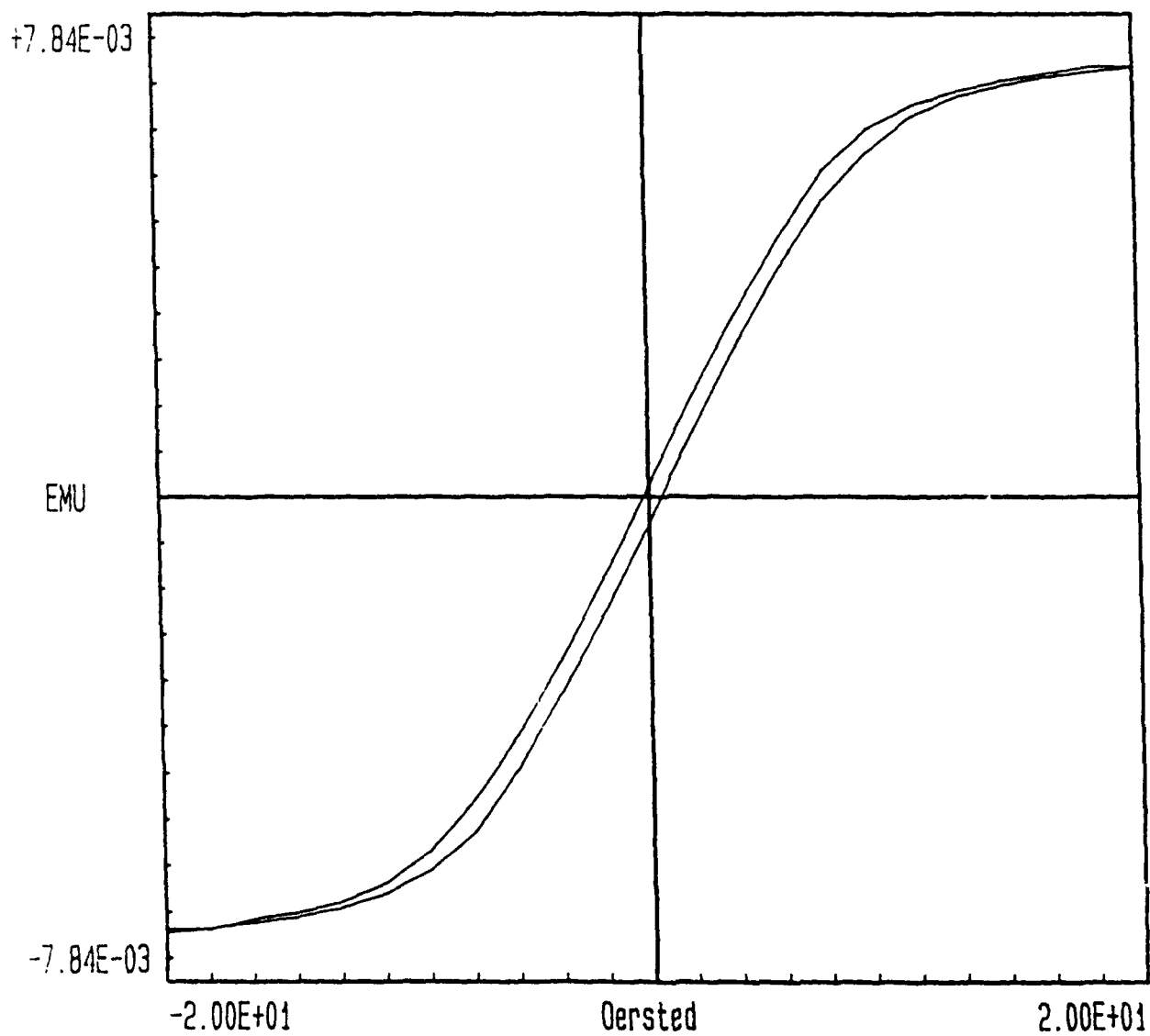


Fig.9 The horizontal axis is expanded for the plot in Fig.8.

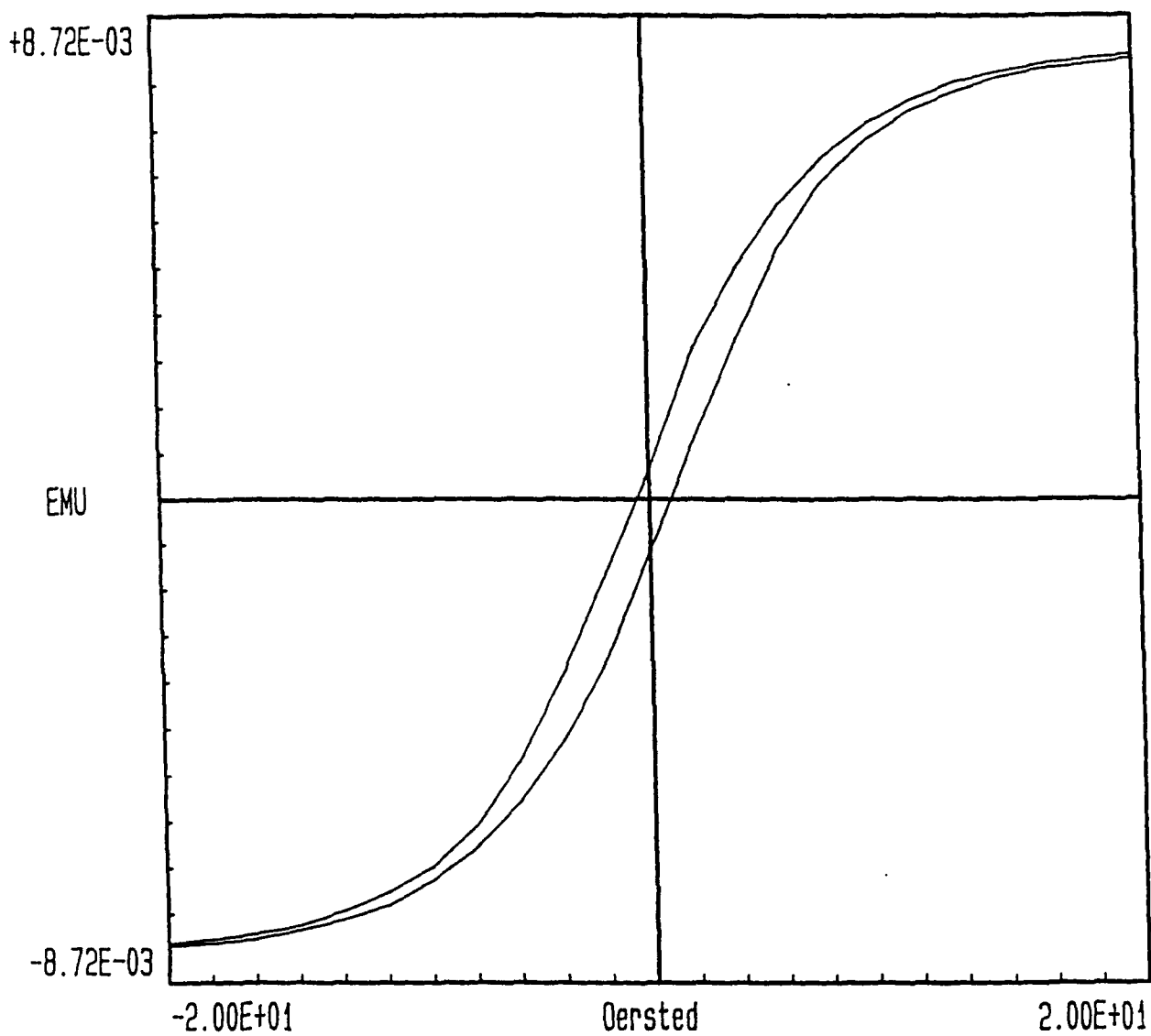


Fig.10 Sample plot as Fig.9 except data is obtained on another sample.

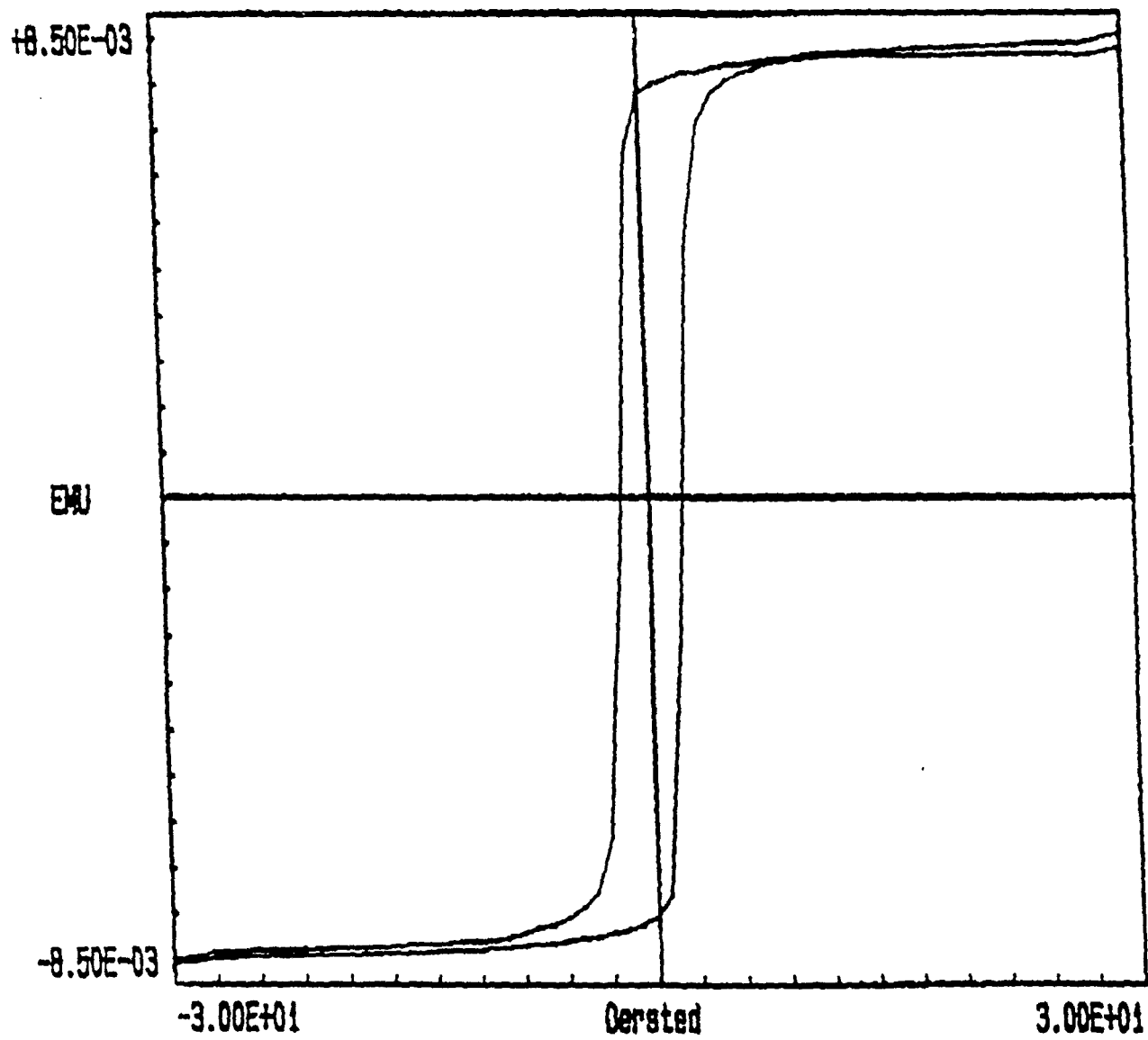


Fig.11 Magnetization is plotted as a function of H for H along the hard axis. The data was obtained after the annealing pulsed field of Fig.5.

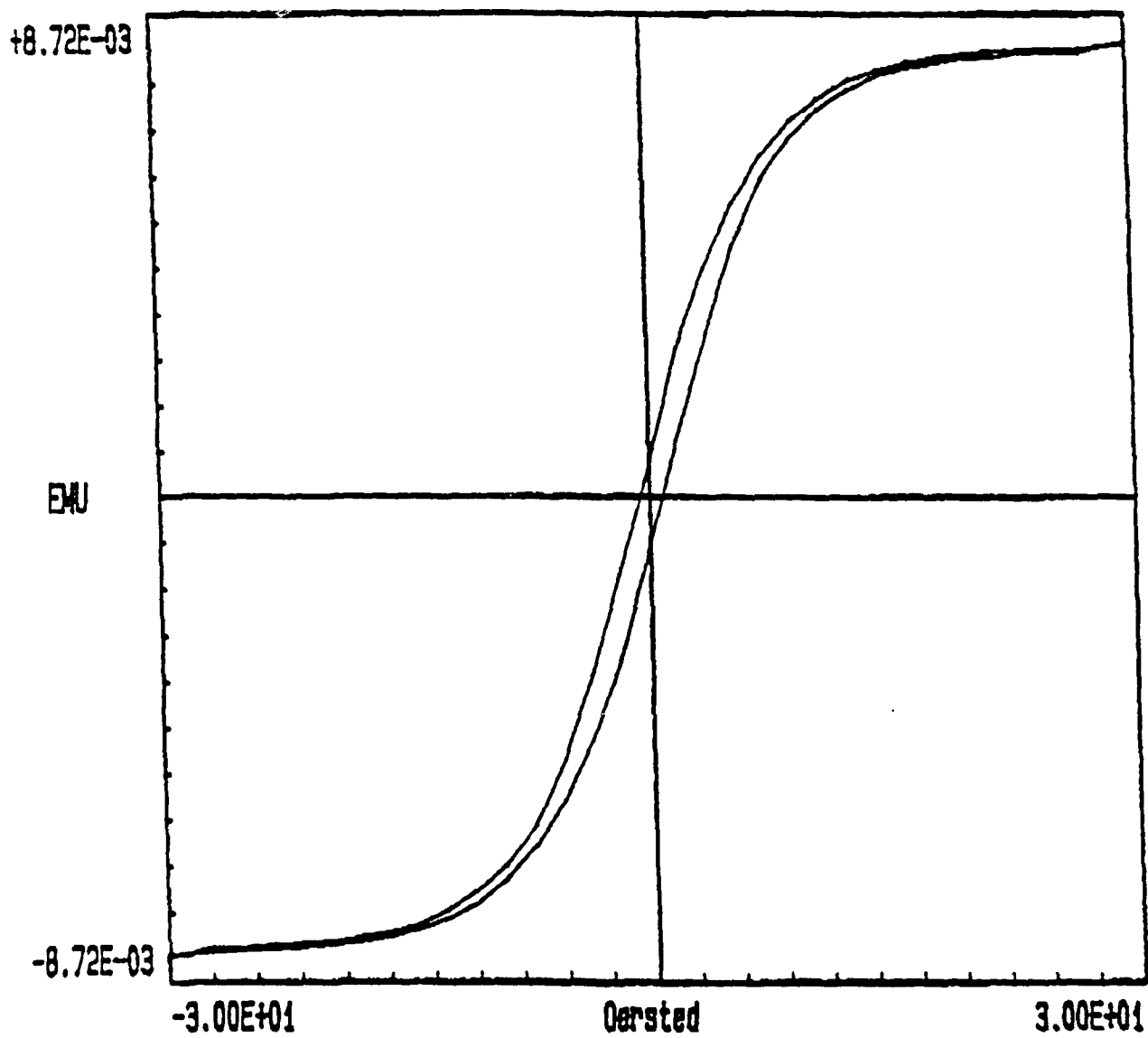


Fig.12 Magnetization versus H on a virgin film of $\text{Fe}_{80}\text{B}_{15}\text{Si}_5$.

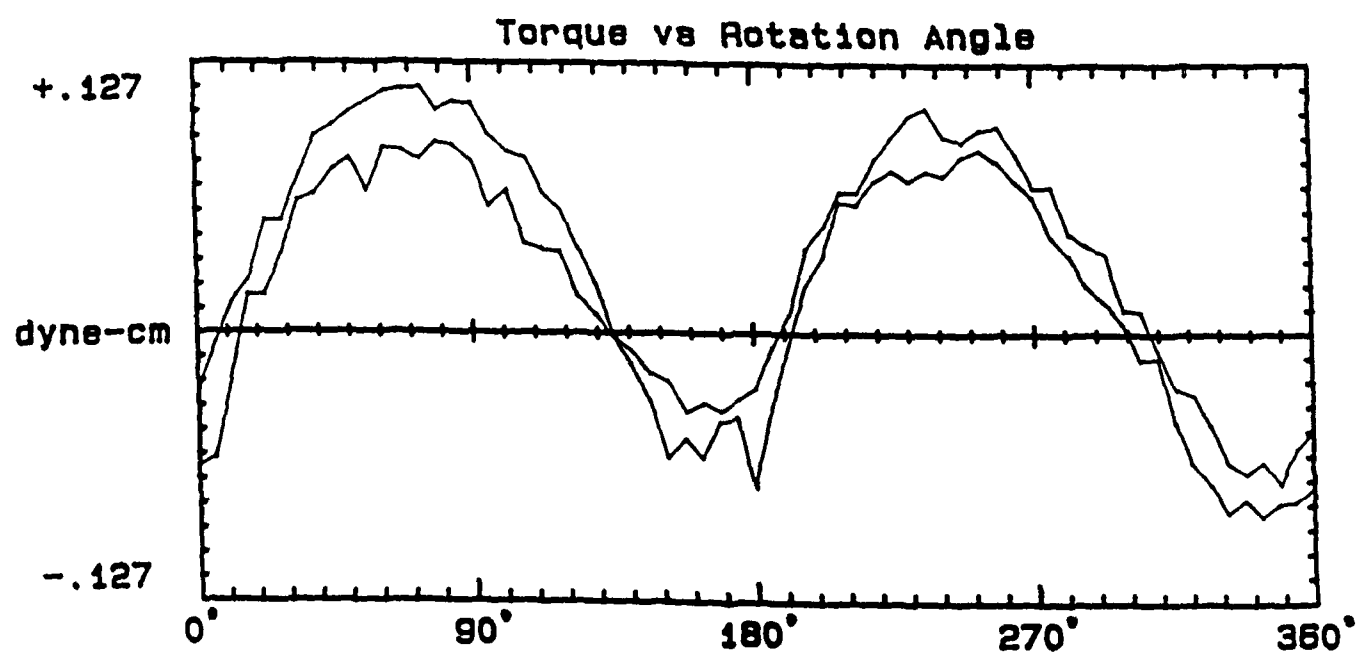


Fig.13 Torque versus field angle on the same sample of Fig.12.

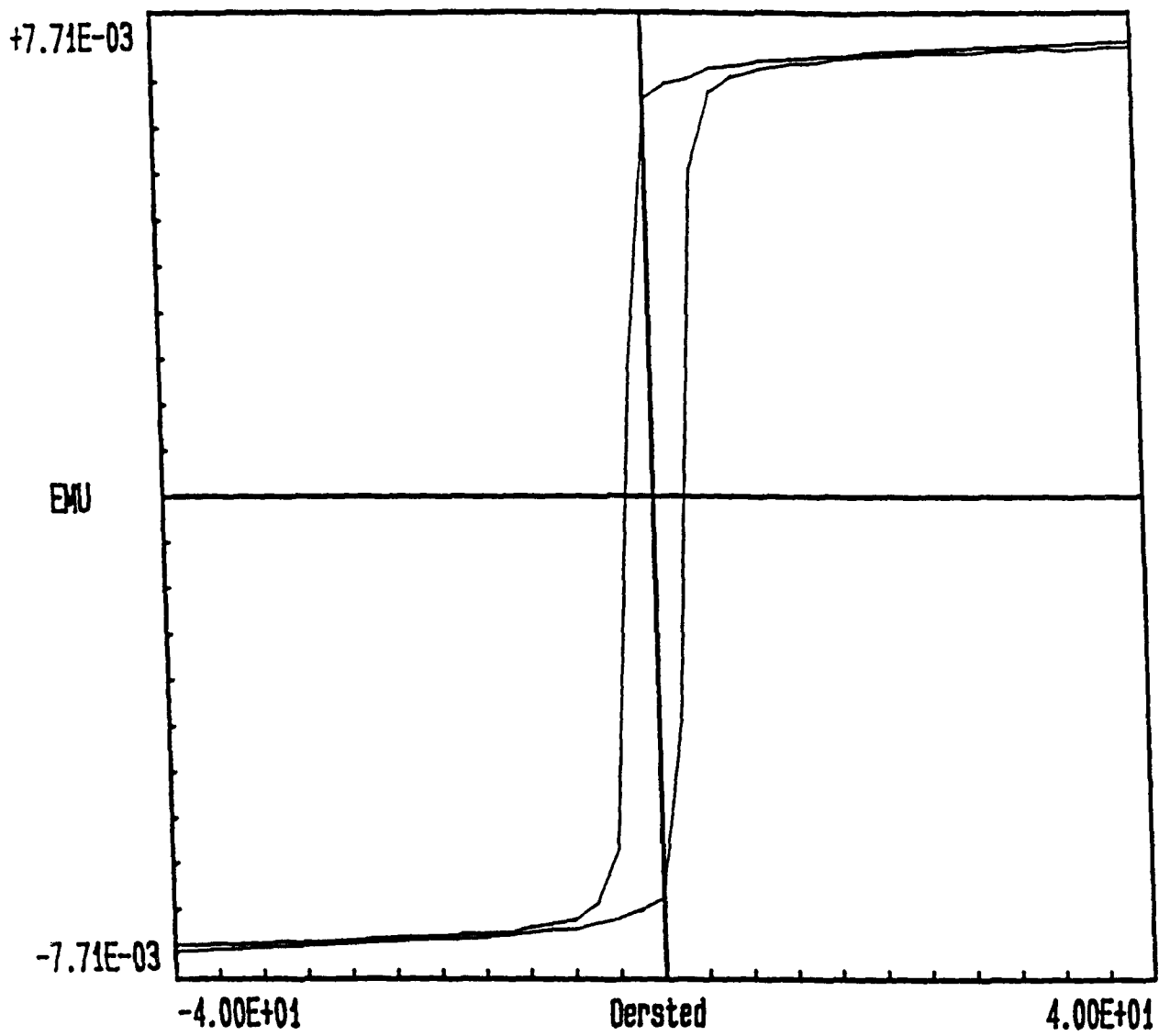


Fig.14 Magnetization versus H (after annealing)

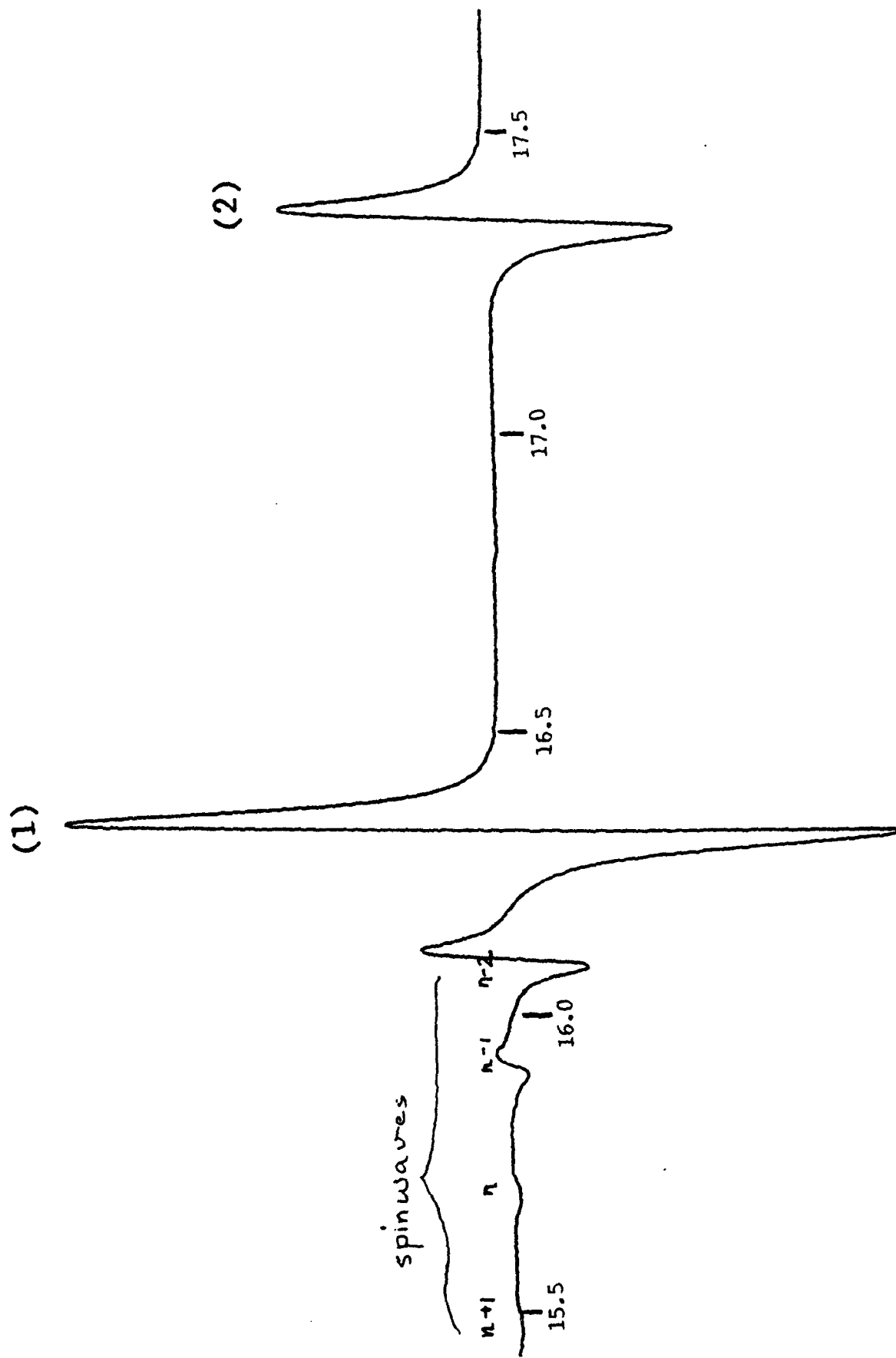


Fig.15 The derivative FMR absorption is plotted as a function of H for H normal to the film plane. The line marked (1) is due to single phase excitation of $\text{FeO}_{0.15}\text{Si}_{0.85}$ or the usual Kittel uniform precessing resonance. Line (2) is due to some form of magnetic segregation which is iron rich.

	SQ ($= M_R/M_S$)		H_A (Oe)		H_c (Oe)	
	before annealing	after annealing	before annealing	after annealing	before annealing	after annealing
Post Annealing Procedure	-0	0.90	13	1.5	0.77	2.1
In-Situ Annealing Procedure	-0	0.87	14	2.0	0.43	2.7

Table I Summary of Annealing Studies.

	$\Delta H(\text{Oe})$	g	$4\pi M(\text{kG})$	$H_A(\text{Oe})$	$f_{\text{res}}(\text{GHz})$
$\text{Fe}_{80}\text{Si}_{15}\text{B}_5$	53 ± 3	1.98 ± 0.01	14.80 ± 0.01	11 ± 0.5	1.12

Table II FMR data.

Alloy	radial distance (Å)	coordination number	σ^2_{300} (Å ²)	technique
Co ₇ Fe ₁ B ₁ Si ₁				
Co-Co	2.46	5.7	.0221	xafs'
Co-Co	2.69	8.2	.055 ^a	
Co-B	2.11	2.6	.0113	
Fe ₇ Ni ₁ B ₁ Si ₁				
Fe-Fe	2.48	3.7	.0181	xafs'
Fe-Fe	2.68	7.4	.0543	
Fe-B	2.11	2.3	.0180	
Ni ₁₀ B ₁				
Ni-Ni	2.24	4.3	.0107	xafs
Ni-Ni	2.46	3.0	.0053	
Ni-Ni	2.63	3.9	.0204	
Ni-B	2.11	3.8	.0027	
Fe ₁₀ B ₁				
Fe-Fe	2.56	10.5		x
Fe-B	2.27	2.4		
Fe ₇ B ₃				
Fe-Fe	2.60	10.5		x
Fe-B	2.27	2.4		
Co ₁₀ B ₁				
Co-Co	2.57	10.2		x
Co-B	2.03	3.9		
Ni ₁₀ B ₁				
Ni-Ni	2.55	9.2		x,n
Ni-B	2.12	4.9		
Co ₁₁ P ₁				
Co-Co	2.55	10.1		x,n
Co-P	2.32	2.10		
Fe ₁₀ P ₁				
Fe-Fe	2.61	10.0		xafs
Fe-P	2.32	3.0		
Fe ₇ Co ₁ B ₁ Si ₁				
Fe-Fe	2.51	7±2	.0224	xafs
Fe-Co	2.46	2.2±2	.0112	

Fe ₇ B ₃			
Fe-Fe	2.62	12.2	DRP
Fe-B	2.07	2.07	
Fe ₁₀ B ₁₀			
Fe-Fe	2.57	11.1	DRP
Fe-B	1.9	4.6	
Fe ₈ B ₁₄			
Fe-Fe		10.97	DRP
Fe-B		1.94	
Fe ₁₀ B ₂₀			
Fe-Fe		10.79	DRP
Fe-B		1.51	
Fe ₁₁ B ₁₃			
Fe-Fe		11.25	DRP
Fe-B		1.06	

a this parameter was fixed during fitting procedures
Möss Mössbauer spectroscopy
x x-ray diffraction analysis
n neutron scattering
DRP calculated using dense random packing models
xafs extended x-ray absorption fine structure analysis, unless noted,
data was acquired via transmission
xafs' conversion-electron extended x-ray absorption fine structure
analysis

References: (10) and (11).

Table III Summary of EXAFS data.

$\text{Fe}_{80}\text{B}_{15}\text{Si}_5$	$M_s(\text{G})$	$A(10^{-6}\text{erg/cm})$	$T_c(\text{K})$	$H_A(\text{Oe})$	$\Delta H(\text{Oe})$
Estimated Values	1490	1.26	515 ± 150	30	14
Measured Values	1450	0.90	624	13-15	30

Table IV Comparison of estimated and Measured magnetic parameters.